JCSE The Journal of Corrosion Science and Engineering

ISSN 1466-8858

Volume 7 Preprint 107

Breakdown of Anodic Films on Titanium and its Suppression by Alloying

H. Habazaki, M. Uozumi, H. Konno
Graduate School of Engineering, Hokkaido University, Sapporo 060-8628, Japan, Habazaki@eng.hokudai.ac.jp
K. Shimizu
University Chemical Laboratory, Keio University, Hiyoshi 4-1-1, Yokohama 223-8521, Japan
P. Skeldon, G.E. Thompson, G.C. Wood
Corrosion and Protection Centre, UMIST, P.O. Box 88, Manchester M60 1QD, UK

Abstract

Breakdown of anodic films on titanium, associated with their crystallization, and influences of alloying additions on the crystallization have been examined by transmission electron microscopy of ultramicrotomed sections, combined with Rutherford backscattering spectroscopy and glow discharge optical emission spectroscopy. Anodic oxide films have been formed on sputter-deposited titanium and its alloys containing a range of valve metals at a constant current density of 50 A m^{-2} in 0.1 mol dm^{-3} ammonium pentaborate electrolyte. In the case of titanium, anatase develops at relatively low voltage in the inner film region, formed by anion ingress.

In contrast, the outer film region, formed at the film/electrolyte interface, is composed only of amorphous oxide. Oxide crystals are found near the plane separating the two regions, which is located at a depth of 35-38% of the film thickness. Oxide zones, of size ~ 1 nm, with a relatively ordered structure, developed at the metal/film interface, are considered to lead to transformation of the inner region structure. Incorporation into the film of alloying element species, such as aluminium, molybdenum, silicon and zirconium species, suppresses the crystallization such that uniform amorphous anodic oxides can grow to high voltages. However, the effectiveness of the suppression of crystallization is dependent upon the particular alloying element species; small amounts of alloying elements that form oxides with strong metal-oxygen bonds tend to suppress the crystallization more effectively.

Keywords: Anodic titania, crystallization, anatase, ionic transport, TEM

Introduction

Titanium is one of the more important engineering metals, partly due to its bio-compatibility and high corrosion resistance. Of relevance to these properties, anodic films formed on titanium have been examined extensively. Various electrochemical investigations, including ac impedance spectroscopy, photoelectrochemistry and scanning electrochemical microscopy, in addition to ellipsometric studies, have demonstrated the changes in the growth behaviour and film properties with anodizing conditions [1-10]. The dependence of film properties on the grain orientation of the titanium substrate has been also reported [11-15]. From these investigations, it is known that an amorphous-to-crystalline transition occurs on titanium at relatively low voltages of ~10 V, in contrast to growth of amorphous oxides on aluminium and tantalum to high voltages. Crystallization of the anodic films on titanium induces electron-conducting paths, allowing oxygen evolution on crystalline regions to occur, which has been associated with the breakdown of the film [16].

Direct evidence of the formation of crystalline oxide on titanium has been obtained by in-situ and ex-situ Raman spectroscopy [17-20] and

transmission electron microscopy (TEM) [20, 21]. Most studies have demonstrated the transformation of amorphous oxide to anatase, with rutile forming at increased voltages. Although an electrostriction model has been proposed [20], the precise mechanism of crystallisation is uncertain, partly due to lack of information about the in depth distribution of crystalline oxides in the films.

In this paper, recent investigations by the authors of the crystallization of anodic titania, studied using TEM, and its suppression by alloying additions, such as aluminium, molybdenum, silicon and zirconium, have been considered further in order to gain insight into the mechanism of crystallisation.

Experimental

Layers of titanium, and titanium alloys containing various concentrations of aluminium, molybdenum, silicon and zirconium, 200-300 nm thick, were prepared by d.c. magnetron sputtering using a 99.9% pure titanium target, with small pieces of alloying elements placed on the sputter-erosion region for preparation of alloys. The sputtering chamber was firstly evacuated to $<1 \times 10^{-5}$ Pa, with deposition carried out in 99.999% argon at about 2×10^{-1} Pa. The compositions of the alloys were determined by Rutherford backscattering spectroscopy (RBS) using 2.0 MeV He^{2+} ions. The scattered ions were detected at 170° to the incident beam direction, which was normal to the specimen surface. The data were analysed using the RUMP program.

Specimens were anodized at a constant current density of 50 A m^{-2} to selected voltages in various stirred electrolytes at 293 K. Electron transparent sections, of nominal thickness 10 nm, of anodized specimens were then prepared using a Leica Ultracut-S ultramicrotome for subsequent observation by TEM in a JEOL JEM-2000FX instrument operating at 200 kV.

Elemental depth profiling of the anodic films was carried out by r.f. glow discharge optical emission spectroscopy (GDOES) using a Jobin Yvon 5000 rf instrument in an argon atmosphere of 538 Pa by

applying r.f. of 13.56 MHz and power of 40 W. The signals were detected from an area of 4 mm diameter.

Results and Discussion

Voltage-time responses of titanium in various electrolytes

Voltage-time curves of the sputter-deposited titanium during anodizing in various electrolytes are shown in Fig. 1. In all electrolytes, except for 14.6 M phosphoric acid, the voltage increases linearly with time to only about 10 V, after an initial voltage surge of about 2 V at the commencement of anodizing. Then, a progressive increase in the slope is observed, and finally, the voltage increases relatively slowly. In the case of anodizing in sodium tungstate electrolyte, a sudden drop in voltage marks the commencement of the region of slow voltage rise. In the final stage, gas evolution was evident on the surface of the specimens. During anodizing in 14.6 M phosphoric acid electrolyte, the voltage increases linearly with time to a slightly higher voltage of about 45 V, and then increases more slowly with gas evolution from the surface. Thus, unlike aluminium and tantalum, uniform film growth on titanium to high voltages is not achieved.

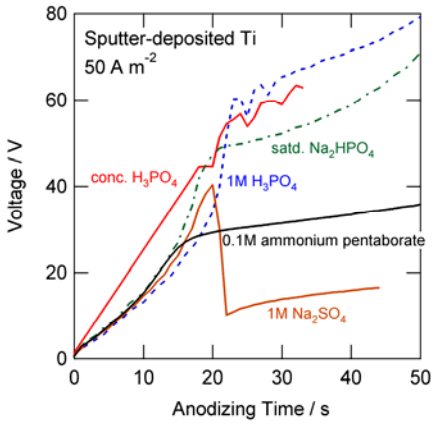

Fig. 1 Voltage-time curves of the sputter-deposited titanium during anodizing at 50 A m^{-2} in various electrolytes at 293 K.

SEM and TEM observations of anodic films on titanium

Scanning electron microscopy of the surface of titanium, anodized to 80 V, revealed the presence of many cavities and swellings, associated with gas evolution [22]. Thus, gas should be generated, not from the

surface of the oxide film, but within the oxide film. Figure 2 shows a transmission electron micrograph of a stripped anodic film formed to 20 V in 0.1M ammonium pentaborate electrolyte. The film was stripped by immersing the titanium specimen anodized to 20 V in bromine-methanol solution. The micrograph reveals bubble-like features, possibly associated with oxygen generation even at this low voltage. The generation of gas, within the anodic film, may be one of the reasons for the progressive increase in the slope in the voltage-time response (Fig. 1). The selected area electron diffraction pattern, shown in Fig. 2, corresponds to anatase, such that an amorphous-to-crystalline transition occurs below 20 V. Similar images can be seen by using high-resolution, low voltage scanning electron microscopy (Fig. 3). The left- and right-side images were obtained using out-lens and in-lens detectors respectively. The regions with light appearance on the right appear dark on the left, possibly due to the presence of oxygen gas in the region. The formation of crystalline oxide in the film formed to 20 V is confirmed further by TEM of an ultramicrotomed section (Fig. 4). The film is of thickness ~ 35-40 nm, with irregular film/electrolyte and metal/film interfaces associated mainly with the rough surface of the as-deposited titanium. Lattice fringes, with spacing of ~ 0.35 nm, are revealed in the middle of the anodic film, indicating nanocrystals of anatase, in agreement with the electron diffraction pattern in Fig. 2. Further, nanoscale bubbles have developed around the nanocrystals, due to local generation of oxygen. The outer 30% of the film is composed of an amorphous oxide, with no

lattice fringes evident.

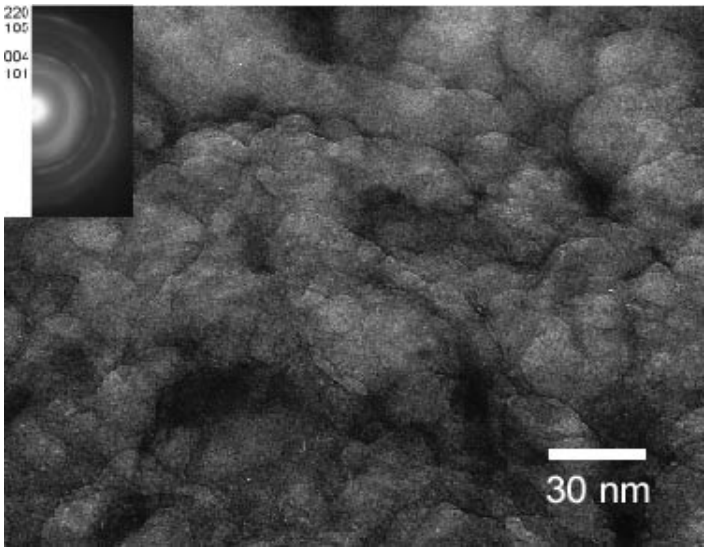

Fig. 2 Transmission electron micrograph of a stripped anodic film formed on sputter-deposited titanium to 20 V in 0.1 M ammonium pentaborate electrolyte at 293 K.

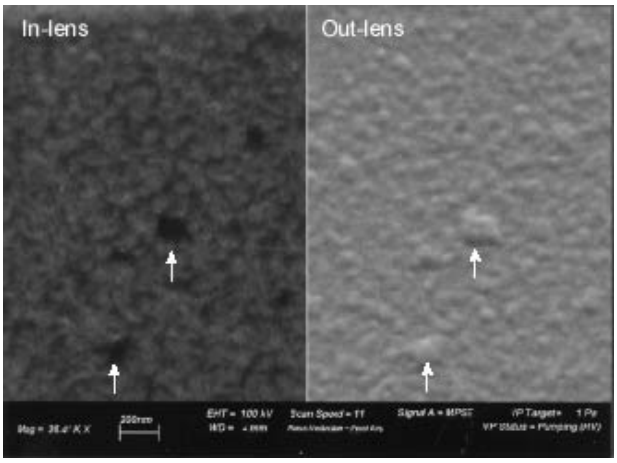

Fig. 3 Low voltage, high-resolution scanning electron micrographs of the sputter-deposited titanium anodized to 20 V in 0.1 M ammonium pentaborate electrolyte at 293 K.

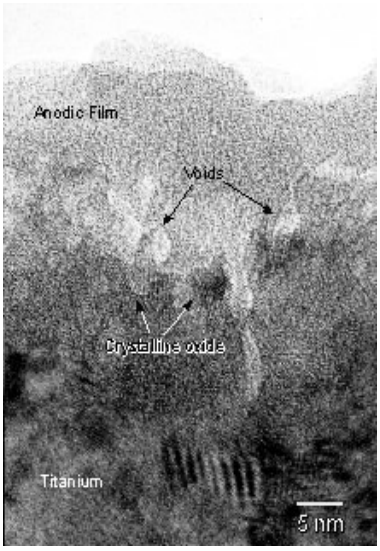

Fig. 4 Transmission electron micrograph of an ultramicrotomed section of the sputter-deposited titanium anodized to 20 V in 0.1 M ammonium pentaborate electrolyte at 293 K.

The distribution of the oxide crystals can be correlated with ionic transport during film growth. Amorphous titania is formed both at the film/electrolyte and metal/film interfaces by cation egress and anion ingress respectively, with the transport number of cations being 0.35-0.38 [23-25]. Electrolyte-derived species are incorporated in to the outer part of anodic films and stabilize the amorphous structure [26, 27]. In the present film, boron species are distributed in the outer

~19% of the film due to their outward migration [24]. Amorphous titania, free of boron species, is present below the boron-containing film region. Hence, the formation of amorphous material in the film region generated at the film/electrolyte interface is not only due to the presence of boron species.

In contrast to the amorphous structure of the outer layer, the inner film layer, formed at the metal/film interface by the inward migration of O^{2-}/OH^{-} ions, contains nanocrystals. Their formation may be associated with oxide regions with a relatively ordered structure, of size ~1 nm, formed at the metal/film interface, that arise due to the structure of the metal, impurity elements in the substrate and growth stresses at the interface [28]. Contributions may also arise from electrostriction [20]. Ionic transport, under an electric field of ~5 x 10^{8} V m^{-1}, should favour crystal growth at sites of early nucleation now located at 35-38% of the film thickness presuming that the crystals are immobile, similar to γ-Al_2O_3 nuclei in anodic alumina [29]. As will be evident from later consideration of alloys, immobile precursor nuclei may also be present at this depth. In general, crystalline oxides have higher ionic resistivities, and hence higher electric fields than the corresponding amorphous oxides [29]. Thus, the probability of excitation of electrons in the valence band, formed by overlapping of O 2p orbitals in crystalline titania, to the conduction band is enhanced, leading to the oxidation of O^{2-} ions to form O_2 molecules and later development of bubbles. The growth of the anodic film on titanium is illustrated schematically in Fig. 5.

5.

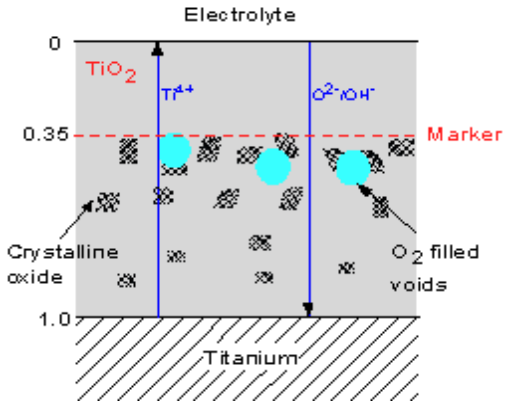

Fig. 5 Schematic diagram illustrating the formation of crystalline oxide in an anodic film on titanium.

Influence of alloy additions on the structure of anodic titania

As described above, incorporated foreign species in anodic films generally stabilize the amorphous structure. Since oxide crystals are developed in the inner part of anodic titania film, where the film materials are formed at the metal/film interface, it is readily expected that incorporation of foreign species in the inner region of anodic titania stabilises the amorphous structure, resulting in uniform film growth to high voltages. The incorporation in to this region can be achieved readily by alloying of titanium; the alloying element species should distribute at least throughout the film region formed at the alloy/film interface, unless the species are mobile inwards.

Here, an example of the addition of aluminium to titanium is revealed. Figure 6 shows voltage-time responses of the sputter-deposited titanium and Ti-Al alloys, with several aluminium contents, during anodizing in 0.1 M ammonium pentaborate electrolyte. It is evident that the linear voltage increase, suggesting uniform film growth, extends to higher voltages with an increase of the aluminium content in the alloy. After the linear voltage increase, all the alloys reveal progressive increase in the slope and subsequent dielectric breakdown,

at which sparking and gas evolution were evident.

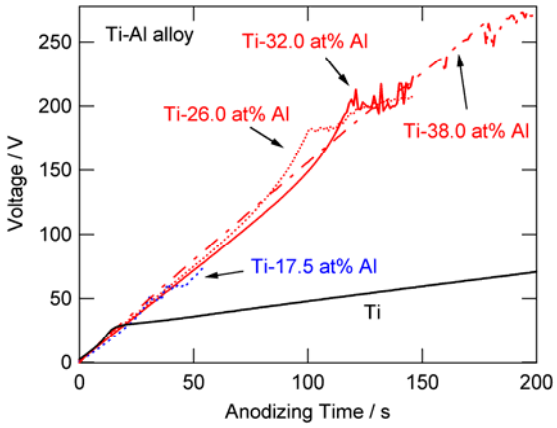

Fig. 6 Voltage–time curves of sputter-deposited titanium and Ti–Al alloys with several compositions during anodizing at 50 A m^{-2} in 0.1 M ammonium pentaborate electrolyte at 293 K.

Growth of uniform anodic films during the linear voltage increase has been confirmed by TEM observations. An example of a transmission electron micrograph of an ultramicrotomed section of the Ti–26.0 at% Al alloy anodized to 50 V is given in Fig. 7. Unlike the film formed on titanium (Fig. 4), the anodic film formed on this alloy, with flat and parallel alloy/film and film/electrolyte interfaces, does not contain bubbles and is apparently featureless, indicating the amorphous structure. The thickness of the film is 100 ± 3 nm, corresponding to a formation ratio of 2.0 nm V^{-1}A. A similar uniform film, of 178 ± 3 nm thickness, was formed on the Ti–38.0 at% Al alloy to 100 V, with a corresponding formation ratio of about 1.8 nm V^{-1}. Thus, the increased aluminium content reduces the formation ratio, due to the smaller formation ratio of anodic alumina, i.e., 1.2 nm V^{-1} [30], compared with that of anodic titania, about 2.0 nm V^{-1} [31].

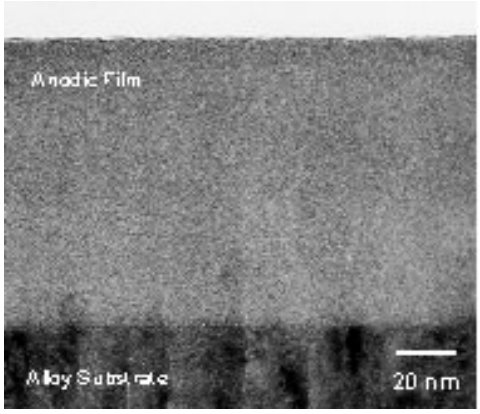

Fig. 7 Transmission electron micrograph of an ultramicrotomed section of the sputter-deposited Ti-26 at% Al alloy anodized to 50 V in 0.1 M ammonium pentaborate electrolyte at 293 K.

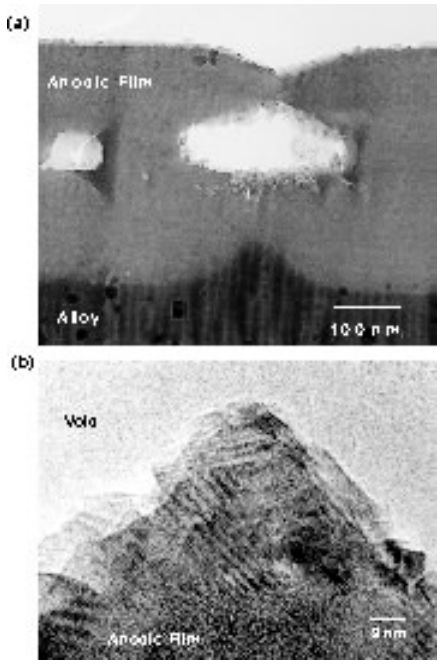

Fig. 8 Transmission electron micrograph of an ultramicrotomed section of the sputter-deposited Ti-26 at% Al alloy anodized to 160 V in 0.1 M ammonium pentaborate electrolyte at 293 K.

In the region where progressive increase of the slope in the voltage-time curves is observed, formation of nanocrystals and voids within

the anodic films has been found, as shown in the example of the Ti-26.0 at% Al alloy that had been anodized to 160 V (Fig. 8). Relatively large voids, associated with oxygen generation, are formed at ~40% of the film thickness from the film/electrolyte interface. From the high resolution image (Fig. 8(b)), formation of nanocrystals, with lattice spacing of 0.35 nm, is evident in the vicinity of voids. The film region containing nanocrystals and voids, possibly filled with oxygen, is located close to the plane separating film regions formed at the alloy/film interface by anion ingress and at the film/electrolyte interface by cation egress, since the transport numbers of cations in amorphous anodic alumina (~0.4) and in amorphous anodic titania (0.35-0.38) are similar. GDOES depth profiles of the anodic film formed on the Ti-32.0 at% Al to 100 V (Fig. 9) reveals that both titanium and aluminium ions are distributed throughout the film thickness. The wavy profiles of titanium and aluminium in the films are due to optical interference of light emitted from the respective elements. The steeper increase in the titanium profile at the film surface, compared with that of aluminium, suggests formation of a thin outer layer of TiO_2 due to titanium ions migrating slightly faster than aluminium ions. Incorporation of boron species in the outer 32% of the film is evident, indicating its outward mobility in growing film. The composition of the anodic film was also confirmed from RBS analysis, indicating that the anodic films formed on the Ti-26 at% Al and Ti-32.0 at% Al alloys to 100 V mainly consist of uniformly distributed units of Al_2O_3 and TiO_2. The resolution of RBS was insufficient to identify any thin outer layer of TiO_2. From these results, the formation of nanocrystals at about 40% of film thickness from the film/electrolyte interface cannot be attributed to a differing composition in this region.

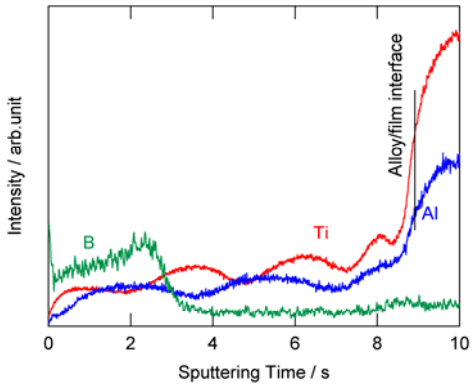

Fig. 9 GDOES depth profiling analysis of the anodic film formed on the sputter-deposited Ti-32 at% Al alloy to 100 V in 0.1 M ammonium pentaborate electrolyte at 293 K.

Development of bubbles and crystalline oxide at the film region close to the plane separating film regions formed by anion ingress and cation egress is also evident for Ti-6 at% Si [32] and Ti-10.5 at% Zr alloys [33]. From these results, it is likely that pre-cursor nuclei exist in the air-formed oxide. These pre-cursors are immobile in the anodic film and may arise due to reaction of the alloys and titanium with residual oxygen in the sputtering chamber. During sputtering, substrates are heated to ~ 373 K by the sputtering process, with pre-cursor nuclei possibly developing during cooling of substrates. Ageing of the as-deposited Ti-6 at% Si alloy in laboratory atmosphere for one month promotes the crystallization of the anodic film. During ageing of the alloy, crystal nuclei, that are immobile during anodic film growth, probably develop in the air-formed film [32].

Formation of crystalline oxides in anodic titania can be suppressed up to high voltages by incorporation of sufficient amounts of alloying element species from the substrates. As described above, the linear voltage increase with anodizing time for the Ti-Al alloys extends to higher voltages with increased aluminium content in the alloy (Fig. 6). However, the amounts of alloying elements required to suppress the formation of crystalline oxides to high voltages, e.g., 100 V, are strongly dependent upon the particular alloying elements. Figure 10 shows the voltages at which the region of linear voltage increase with time terminates during anodizing at a constant current density, for

several titanium alloys. Obviously, silicon is most effective in extending uniform film growth, i.e., suppression of the formation of crystalline oxides, to high voltages, while relatively large amounts of aluminium are required for growth of uniform films to high voltages. From this Figure, the amount of alloying element required to grow uniform films to 100 V increases in the order of silicon, molybdenum, zirconium and aluminium. This order is in approximate agreement with that of the strengths of metal–oxygen bonds of their oxides, i.e., single metal–oxygen bond energies of Si^{4+}–O, Mo^{6+}–O, Zr^{4+}–O and Al^{3+}–O are 465, 359, 276 and 281 kJ mol^{-1} respectively [34]. Aluminium ions incorporated into anodic titania have a similar mobility to titanium ions, such that both cations are distributed throughout most of the film thickness, as described previously. However, other incorporated alloying element species have mobilities different from that of titanium ions. The authors have found that there is a good correlation between the mobilities of outwardly mobile incorporated species in anodic amorphous titania [24], as well as in anodic alumina [35], and their single metal–oxygen bond energies: species with stronger metal–oxygen bonds migrate more slowly. Thus, it is likely that the alloying element species, which migrate more slowly, and hence are more concentrated in the inner film region relative to the alloy composition, suppress more effectively the formation of crystalline oxides in anodic titania. The amorphous-to-crystalline transition of anodic titania involves local re-ordering of ionic arrangements, which is possibly assisted by ionic transport during film growth under the high electric field. The slower migrating species may impede such ordering of ionic arrangements, and hence, the amorphous structure of anodic oxides is sustained to high voltages.

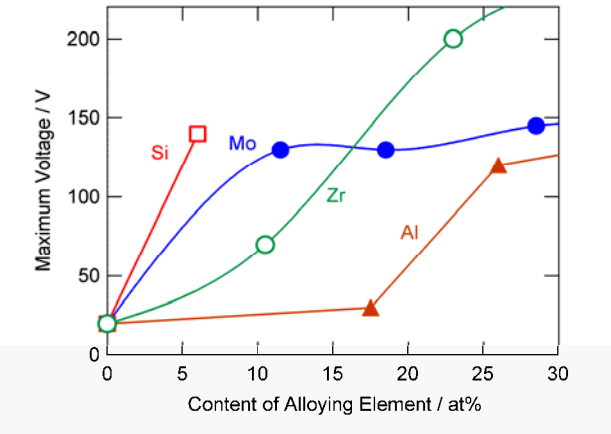

Fig. 10 Compositional dependence of the maximum voltage for the linear voltage increase in the voltage–time response of the titanium alloys during anodizing at 50 A m^{-2} in 0.1 M ammonium pentaborate electrolyte at 293 K.

Conclusions

An amorphous-to-crystalline transition of anodic oxide formed on titanium occurs during anodizing in 0.1 M ammonium pentaborate electrolyte to ~20 V. Oxide crystals, which consist of anatase, develop in the film region where film materials are formed at the metal/film interface by anion ingress, while the remaining outer region formed at the film/electrolyte interface by cation egress consists only of amorphous oxides. Oxide zones, of size ~ 1 nm, with a relatively ordered structure, developed at the metal/film interface, are considered to lead to transformation of the inner region structure. The incorporation of foreign species from the substrate suppresses the amorphous-to-crystalline transition, resulting in the uniform film growth to high voltages. Species incorporated from the substrate, such as aluminium, molybdenum, silicon, and zirconium species, are distributed at least throughout the film region formed by anion ingress, which cannot be achieved by electrolyte-derived species. The slower migrating species, with stronger metal-oxygen bonds, that impede local re-ordering of ionic arrangements, suppress more effectively the formation of oxide crystals.

Acknowledgments

Thanks are due to Mr.Y.Uchida of Horiba Ltd., Tokyo, Japan for the provision of time on Jobin Yvon 5000 RF GDOES instrument. The present work was supported in part by the Light Metal Educational Foundation, Inc.

References

1. 'Changes in electrochemical properties of the anodic oxide film formed on titanium during potential sweep', K. Azumi and M. Seo, *Corrosion Science*. **43**, 533, 2001.
2. 'The influence of growth rate on the properties of anodic oxide films on titanium', D.J. Blackwood and L.M. Peter, *Electrochimica Acta*. **34**, 1505, 1989.
3. 'An ellipsometric study of the growth and open-circuit dissolution of the anodic oxide film on titanium', D.J. Blackwood, R. Greef, and L.M. Peter, *Electrochimica Acta*. **34**, 875, 1989.
4. 'Modelling of the impedance behaviour of an amorphous semiconductor schottky barrier in high depletion conditions. Application to the study of the titanium anodic oxide/electrolyte junction', C. da Fonseca, M. Guerreiro Ferreira, and M. da Cunha Belo, *Electrochimica Acta*. **39**, 2197, 1994.
5. 'The photoelectrochemistry of thin passive layers. Investigation of anodic oxide films on titanium metal', F. Di Quarto, S. Piazza, and C. Sunseri, *Electrochimica Acta*. **38**, 29, 1993.
6. 'Local film thickness and photoresponse of thin anodic TiO_2 films on polycrystalline titanium', M. Kozlowski, W.H. Smyrl, L. Atanasoska, and R. Atanasoski, *Electrochimica Acta*. **34**, 1763, 1989.
7. 'A photoelectrochemical and ac impedance study of anodic titanium oxide films', J. Marsh and D. Gorse, *Electrochimica Acta*. **43**, 659, 1998.
8. 'The dependence of the optical property of Ti anodic oxide film on its growth rate by ellipsometry', T. Ohtsuka and N. Nomura, *Corrosion Science.* **39**, 1253, 1997.

9. 'The influence of the growth rate on the semiconductive properties of titanium anodic oxide films', T. Ohtsuka and T. Otsuki, *Corrosion Science.* **40**, 951, 1998.
10. 'Reactivation of passive titanium: the enhancement of O_2 evolution after potentiodynamic cyclings', E.M. Oliveira, C.E.B. Marino, S.R. Biaggio, and R.C. Rocha-Filho, *Electrochemistry Communications*. **2**, 254, 2000.
11. 'Anisotropy micro-ellipsometry for in-situ determination of optical and crystallographic properties of anisotropic solids and layers with Ti/TiO_2 as an example', A. Michaelis and J.W. Schultze, *Thin Solid Films*. **274**, 82, 1996.
12. 'Effect of texture and formation rate on ionic and electronic properties of passive layers on Ti single crystals', S. Kudelka, A. Michaelis, and J.W. Schultze, *Electrochimica Acta*. **41**, 863, 1996.
13. 'Photoelectrochemical imaging and microscopic reactivity of oxidised Ti', S. Kudelka and J.W. Schultze, *Electrochimica Acta*. **42**, 2817, 1997.
14. 'Heterogeneous growth of anodic oxide film on a polycrystalline titanium electrode observed with a scanning electrochemical microscope', K. Fushimi, T. Okawa, K. Azumi, and M. Seo, *J. Elelctrochemical Society.* **147**, 524, 2000.
15. 'A scanning electrochemical microscopic observation of heterogeneous oxygen evolution on a polycrystalline titanium during anodic oxidation', K. Fushimi, T. Okawa, and M. Seo, *Electrochemistry*. **68**, 950, 2000.
16. 'Breakdown and efficiency of anodic oxide growth on titanium', C.K. Dyer and J.S.L. Leach, *J. Electrochemical Society.* **125**, 1032, 1978.
17. 'Raman spectra of the anodic oxide film on titanium in acidic sulfate and neutral phosphate solutions', T. Ohtsuka, J. Guo, and N. Sato, *J. Electrochemical Society.* **133**, 2473, 1986.
18. 'Raman spectroscopy of titanium dioxide layers', A. Felske and W.J. Plieth, *Electrochimica Acta*. **34**, 75, 1989.
19. 'In situ Raman spectra of anodically formed titanium dioxide layers in solutions of H_2SO_4, KOH and HNO_3', L.D. Arsov, C. Kormann, and W.Plieth, *J. Electrochemical Society.* **138**, 2964, 1991.

20. 'The effect of film formation conditions on the structure and composition of anodic oxide films on titanium', T. Shibata and Y.-C. Zhu, *Corrosion Science.* **37**, 253, 1995.
21. 'Electrolytic breakdown crystallization of anodic oxide films on Al, Ta and Ti', J. Yaholom and J. Zahavi, *Electrochemica Acta*. **15**, 1429, 1970.
22. 'Influence of molybdenum species on growth of anodic titania', H. Habazaki, M. Uozumi, H. Konno, K. Shimizu, S. Nagata, K. Asami, P. Skeldon, and G.E. Thompson, *Electrochimica Acta*. **47**, 3837, 2002.
23. 'Ionic transport in amorphous anodic titania stabilised by incorporation of silicon species', H. Habazaki, K. Shimizu, S. Nagata, P. Skeldon, G.E. Thompson, and G.C. Wood, *Corrosion Science.* **44**, 1047, 2002.
24. 'Ionic Mobilities in Amorphous Anodic Titania', H. Habazaki, K. Shimizu, S. Nagata, P. Skeldon, G.E. Thompson, and G.C. Wood, *J. Electrochemical Society.* **149**, B70, 2002.
25. 'The anodic oxidation of valve metals-I. Determination of ionic transport numbers by α-spectroscopy', N. Khalil and J.S.L. Leach, *Electrochimica. Acta*. **31**, 1279, 1986.
26. 'Microcrystallinity in X-ray amoephous anodic Ta_2O_5', K. Shimizu, G.E. Thompson, G.C. Wood, and K. Kobayashi, *Phil. Mag. B*. **63**, 891, 1991.
27. 'Electron-beam-induced crystallization of anodic barrier films on aluminium', K. Shimizu, G.E. Thompson, and G.C. Wood, *Thin Solid Films*. **77**, 313, 1981.
28. 'The anodic oxidation of superimposed metallic layers: theory', J.P.S. Pringle, *Electrochimica Acta*. **25**, 1420, 1980.
29. 'A novel marker for the determination of transport numbers during anodic barrier oxide growth on aluminium', K. Shimizu, K. Kobayashi, G.E. Thompson, and G.C. Wood, *Philosophical Magazine B*. **64**, 345, 1991.
30. 'High-resistance anodic oxide films on aluminum', A.C. Harkness and L. Young, *Canadian J. Chemistry.* **44**, 2409, 1966.
31. 'Anodic oxidation of titanium and its alloys', A. Aladjem, *J. Materials Science.* **8**, 688, 1973.

32. 'Crystallization of anodic titania on titanium and its alloys', H. Habazaki, M. Uozumi, H. Konno, K. Shimizu, P. Skeldon, and G.E. Thompson, *Corrosion Science.*, in press, 2003.
33. 'Influences of Structure and Composition on Growth of Anodic Oxide Films on Ti-Zr Alloys', H. Habazaki, M. Uozumi, H. Konno, K. Shimizu, S. Nagata, K. Asami, K. Matsumoto, K. Takayama, Y. Oda, P. Skeldon, and G.E. Thompson, *Electrochimica Acta*, in press, 2003.
34. 'Effects of alloying elements in anodizing of aluminium', H. Habazaki, K. Shimizu, P. Skeldon, G.E. Thompson, and G.C. Wood, *Trans IMF*. **75**, 18, 1997.
35. 'Anodic oxide growth on valve metals - Future prospects', K. Shimizu and K. Kobayashi, *J. Suf. Finish. Soc. Jpn.* **46**, 402, 1995.